Optimum separate confinement structure for midinfrared HgCdTe heterostructure lasers

Jasprit Singh
Department of Electrical Engineering and Computer Science, The University of Michigan, Ann Arbor, Michigan 48109

Ricardo Zucca
Rockwell International Science Center, Thousand Oaks, California 91360

(Received 3 February 1992; accepted for publication 14 May 1992)

A study for the optimization of HgCdTe heterostructure lasers for applications as midinfrared wavelength sources has been carried out. Structures are examined to emit photons at 2.5 and 4.5 μm at 77 K. For the 2.5 μm case, it is found that a quantum-well laser with well width of 200 Å in a separate confinement structure is optimum. For the 4.5 μm case the optimum structure is one with a 1000 Å active region. For the 4.5 μm case the high carrier density at threshold in quantum wells and the consequent high Auger rates do not allow the decrease of threshold current with smaller well sizes. This result is rather general for narrow-gap zinc-blende semiconductors and represents a cautionary warning against the commonly held belief that narrow quantum wells will always improve threshold currents.

I. INTRODUCTION

The $Hg_{1-x}Cd_xTe$ semiconductor system offers a remarkable tunability in the band gap, allowing one to go from zero band gap to a band gap of ~ 1.5 eV.[1] This tunability has of course been a primary reason for the success of this material in the mid- and long-wavelength infrared detector applications.[2] In principle this tunability should also allow HgCdTe to be a versatile semiconductor system for midwavelength infrared lasers. Recently, lasing has been demonstrated in the HgCdTe-based laser system at 2.9, 3.4, and 3.9 μm, and gradual diminution of many of the material and processing problems should allow one to go to longer wavelengths.[3,4]

An important problem for longwavelength lasers is the Auger process, which becomes increasingly important as the band gap shrinks.[5-7] The Auger recombination rate is usually proportional to n^3, where n $(=p)$ is the electron concentration in the laser. It is thus important to operate the laser at a low value of the carrier density at threshold. However, the lowest value of the 3D carrier density is not compatible with the lowest radiative recombination current. For example, for short-wavelength lasers, where the Auger processes are not important, the threshold current is lowest when the active region is a quantum well ($d \leqslant 100$ Å). The 3D carrier density, however, increases as the well size is decreased, as will be clear from the analysis presented here. The threshold current is extremely important especially in lasers operating at midwavelength because a higher threshold current can lead to heating effects which can further increase the Auger processes.

In this paper we examine theoretically the optimum separate confinement structure that leads to the lowest threshold current. We examine the laser structures for emission at 2.5 and 4.5 μm at 77 K. Since measurements of the Auger rates in HgCdTe are few, we use a value measured at longer wavelength and use a scaling approach to obtain the values at 2.5 and 4.5 μm. We find that in the 2.5 μm case, the optimum structure is indeed a quantum-well structure with dimensions of ~ 200 Å. However, in the 4.5 μm case the optimum structure has an active region width of ~ 1000 Å. This occurs because of the competition between the Auger and radiative processes.

In Sec. II we discuss our theoretical formalism and present our results in Sec. III. Concluding remarks are presented in Sec. IV.

II. THEORETICAL FORMALISM

The laser structure we examine is the separate confinement structure shown in Fig. 1. The structure consists of high-band-gap contact regions (the n and p region), a confinement region with a lower band gap, and an active region. The width of the active region is an important variable and in this study we will examine the effect of this width on the laser performance.

Two important processes in the laser are gain and recombination rate. The gain is defined simply by the negative of the net absorption coefficient α (i.e., emission minus absorption),

$$g(h\omega) = -\alpha(h\omega). \quad (1)$$

In the case of an injection laser, the occupation of the conduction and valence bands is given by the quasi-Fermi levels, defined by the relations for the electron and hole density,

$$n = \int_{E_c}^{\infty} N_c(E) f^e(E) dE, \quad (2)$$

$$p = \int_{E_c}^{-\infty} N_h(E)[1 - f^h(E)] dE, \quad (3)$$

where $N_c(E)$ and $N_h(E)$ are the conduction- and valence-band density of states and the f^e and f^n are the distribution functions related to the quasi-Fermi levels μ_e and μ_n by

 © 1992 American Institute of Physics

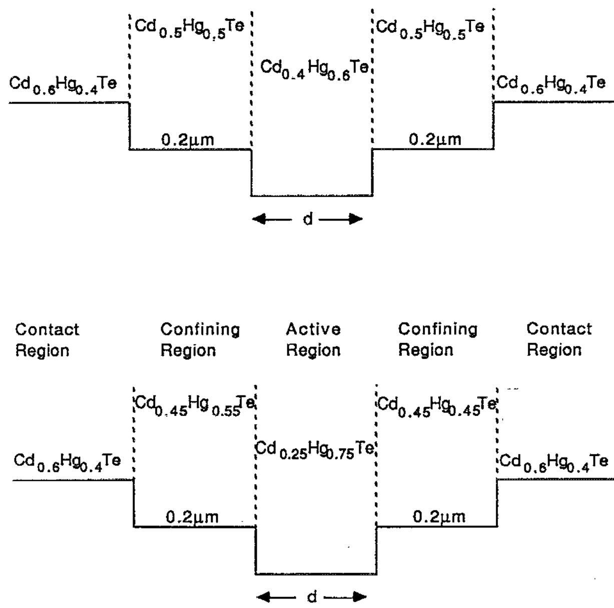

FIG. 1. Separate confinement structures used for the 2.5 and 4.5 μm lasers.

$$f^e(E)=\frac{1}{\exp[(E-\mu_e)/k_BT]+1}, \tag{4}$$

$$f^h(E)=1-\frac{1}{\exp[(E-\mu_h)/k_BT]+1}. \tag{5}$$

The gain spectrum is now given by the emission minus the absorption coefficient (see, for example, Ref. 8 for general formalism and Ref. 9 for specific formalism for quantum-well lasers),

$$g(\hbar\omega)=\frac{4\pi^2e^2\hbar}{\eta_c m^2\hbar\omega}\int\frac{d^3k}{(2\pi)^3}|ap_{if}|^2N_r(E)\{f^e[E^e(k)]-f^h[E^h(k)]\}\delta[E^e(k)-E^h(E)-\hbar\omega]. \tag{6}$$

In case $f^e[E^e(k)]$ is zero and $f^h[E^h(k)]$ is unity, we simply recover the results for the absorption coefficient (with a negative sign). The gain spectrum for the quantum well of size d is given by the expression

$$g_{nm}(h\omega)=\frac{4\pi^2e^2\hbar}{\eta_c m^2 d\hbar\omega}\int\frac{d^2k}{(2\pi)^2}\sum_\sigma|ap_{nm}|^2\{f^e[E^e_n(k)]-f^h[E^h_m(k)]\}\delta[E^e_n(k)-E^h_m(E)-h\omega], \tag{7}$$

where we have used σ to denote the various angular momentum states making up the hole states. In case of the diagonal approximation used here, the mixing of light-hole (LH) and heavy-hole (HH) states is ignored and the summation of σ can be eliminated. The indices n and m denote the electron and hole subband indices. The matrix element is given by

$$p_{nm}=\sum_v\int g^*_n(z)g^v_m(k,z)dz\langle s|p_0|u^h_v\rangle, \tag{8}$$

where the integral over the envelope functions $g_n(z)$, $g_m(z)$ gives approximately unity for $n=m$ and the central cell momentum matrix element is known from the literature. The total gain in the quantum-well structure is obtained by summing the gain from different subband level combinations. A broadening function $\Delta(E)$ is introduced to account for thermal or other inhomogeneous broadening sources. The total material gain is then

$$g(h\omega)=\int dE'\sum_{nm}g_{nm}(E')\Delta(E'-h\omega). \tag{9}$$

The condition for lasing is that the gain should be able to overcome the losses in the cavity, i.e.,

$$\Gamma g=\alpha_{\text{loss}}. \tag{10}$$

The parameter Γ is the optical confinement factor which represents the fraction of optical intensity in the active region. For quantum-well lasers, where the active region is only 50–100 Å, Γ can be quite small (a few percent). The cavity loss is made up of two parts, the loss α_0 due to any absorption in the cladding regions and the loss term arising from the fact that the photons are escaping from the laser facets. If L is the laser cavity length, R is the facet reflectivity, and α_0 the free carrier loss, we have

$$\alpha_{loss}=(1/L)\ln(1/R)+\alpha_0. \tag{11}$$

The optical confinement factor is obtained by solving the optical equation, which takes the form

$$\frac{d^2E_{mk}(z)}{dz^2}+\left(\frac{\epsilon_m(z)\omega^2}{c^2}-k^2\right)E_{mk}(z)=0, \tag{12}$$

where E_{mk} is the z-dependent (confinement direction) electric field, k is the wave number, and $\epsilon_m(z)$ is the z-dependent dielectric constant. The role of the cladding layers is to confine the optical wave by producing a spatial variation in ϵ. The index m represents the waveguide mode.

When electrons and holes are pumped into the conduction and valence bands of a semiconductor, they recombine with each other as we have discussed earlier. In the absence of any photon density in the cavity (i.e., $n=0$), i.e., below threshold, the emission rate is the spontaneous emission rate. The recombination rate per unit area is

$$R_{\text{spon}}=\frac{2}{3}\int d(\hbar\omega)\frac{2e^2\eta\hbar\omega}{m^2c^3\hbar^2}\left(\int\frac{1}{(2\pi)^3}d^3k|p_{if}|^2\times\delta[E^e(k)-E^h(k)-\hbar\omega]\{f^e[E^e(k)]\}\times\{1-f^h[E^h(k)]\}\right)d, \tag{13}$$

where d is the width of the active region.

The integral over $d(\hbar\omega)$ is done to find the rate for all photons emitted, and the integration over d^3k is done to get the rate for all the occupied electron and hole states. The prefactor $\frac{2}{3}$ comes about since we are considering emission into any photon polarization so that we average the matrix element square $|ap_{nm}|^2$ over the polarization vector a.

The extension to quantum-well structures is given by changing the three-dimensional d^3k integral to an integral over the two-dimensional k space,

$$R_{\rm spon}=\frac{2}{3}\int d(\hbar\omega)\,\frac{2e^2\eta\hbar\omega}{m^2c^3\hbar^2}\sum_{nm}\int\frac{d^2k}{(2\pi)^2}\,|p_{nm}|^2 \times\delta[E_n^e(k)-E_m^h(k)-\hbar\omega]\{f^e[E_n^e(k)]\} \times\{1-f^h[E_m^h(k)]\})\,. \qquad (14)$$

In the absence of any nonradiative recombination processes involving either defects or Auger processes, the current flowing in the laser at or below threshold is simply given by

$$J=eR_{\rm spon}. \qquad (15)$$

The laser problem is addressed by a numerical method, where the optical confinement is obtained by discretizing the confinement region and converting Eq. (12) to a difference equation, which is then solved by the matrix method. To calculate the gain and spontaneous emission, we first calculate the band structure of the quantum-well structure. An approach is designed in which the first three subbands are treated by a proper two-dimensional density of states and the higher subbands are represented by a three-dimensional density of states. This allows us to solve the problem for an arbitrary-sized quantum well (e.g., from 50 to 5000 Å). The integrals of Eqs. (7) and (14) are evaluated numerically.

The threshold current, where the lasing action starts, is given by $R_{\rm spon}$ $(n_{\rm th})$, where $n_{\rm th}$ is the carrier concentration at the point where $\Gamma g = \alpha_{\rm loss}$. In the presence of Auger processes, the Auger recombination rate has to be included and the current value increases. We assume that the Auger recombination rates are given by

$$R_{\rm Auger}=Fn^3, \qquad (16)$$

where F is the Auger coefficient. The value of n that is used is the one that results from the solution of Eq. (10), so that the Auger contribution to the threshold current can be evaluated.

III. RESULTS

While our study focuses mainly on the effect of the active well size on the threshold current, we first had to decide on the structure of the separate confinement layer. We chose structures shown schematically in Fig. 1 for the 2.5 and 4.5 μm laser. The 0.2 μm undoped cladding layer was chosen with two objectives: (i) to have as much optical intensity in the active well region as possible and (ii) to have a small fraction $<10\%$ of the optical intensity in the contact regions. The choice of the cladding region is not unique but is a reasonable one for a low-threshold laser. A different choice would not alter our results qualitatively.

In Fig. 2 we plot the optical confinement factor in the active region Γ as a function of the well size. For narrow active region thickness, the optical confinement scales with d. At larger values, it has a weaker dependence on the thickness.

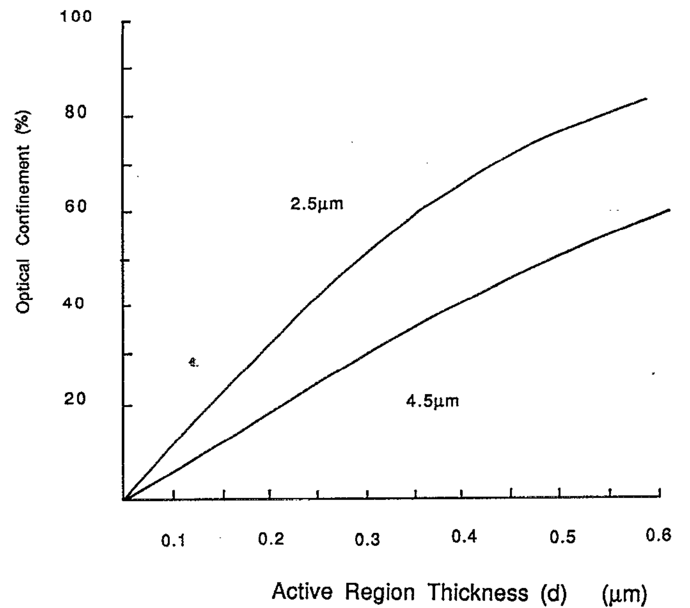

FIG. 2. Optical confinement as a function of the active well region for the 2.5 and 4.5 μm laser.

A. 2.5 μm case

We assume that the cavity loss is 30 cm^{-1} and is independent of the active well size. The cavity loss is due mainly to free-carrier absorption in the contact and cladding layers in the long cavity regime, and should therefore be essentially independent of the active region thickness.

In Fig. 3, we show the peak gain and spontaneous recombination rates as a function of injected two-dimensional carrier densities for two different well sizes. The gain values represent the peak material gain $g(\hbar\omega)$ and are not multiplied by the optical confinement factor. We see from the recombination rate that the e-h recombination time is $\sim$1 ns and has little dependence on the well size. As expected, the peak material gain is much higher when the well size decreases. However, the optical confinement factor also decreases as the well size decreases, and for threshold the product Γg is what is important.

We next examine the threshold 3D carrier density $n_{\rm 3D}$ defined as

$$n_{\rm 3D}=n_{\rm 2D}/d, \qquad (17)$$

where $n_{\rm 2D}$ is the two-dimensional carrier density calculated at threshold. This is plotted as a function of the active region thickness in Figs. 4(a) and 4(b). This quantity is of particular interest since the Auger rates are proportional to the cubic power of the 3D carrier density. As the well size decreases, the carrier density increases rapidly.

We finally examine the radiative and nonradiative currents at threshold for the laser structure as a function of well size. At present, there is no measured value for the Auger coefficient for 2.5 or 4.5 μm. However, there are detailed measurements for E_g = 0.22 eV HgCdTe alloys.

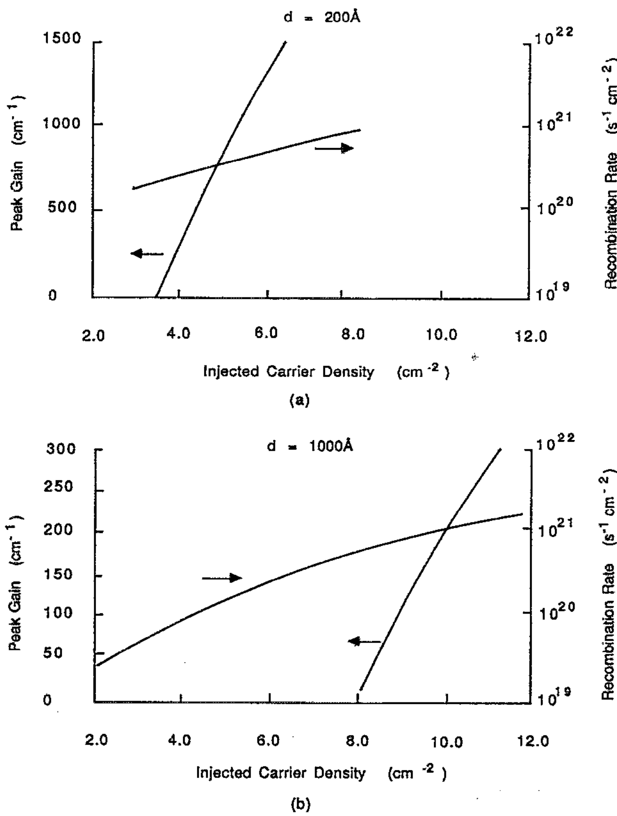

FIG. 3. Peak gain and recombination rates as a function of injected carrier density for (a) 200 Å and (b) 1000 Å active regions laser structures.

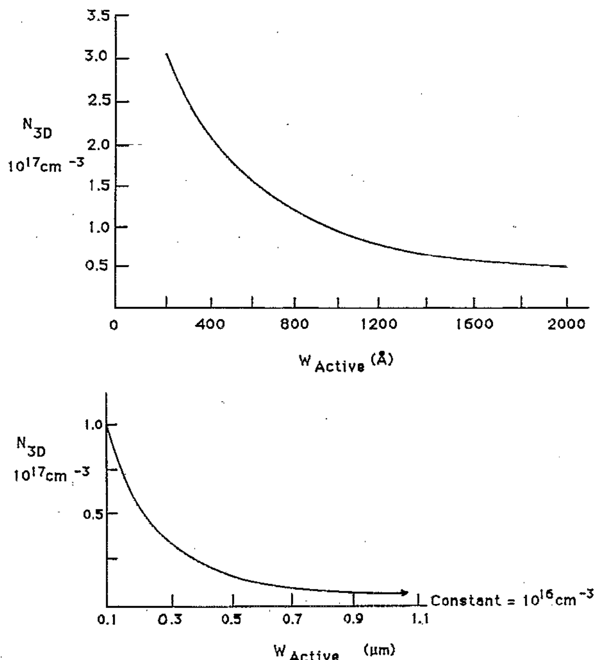

FIG. 4. Variation of the 3D carrier density at threshold as a function of active well size for the 2.5 μm laser.

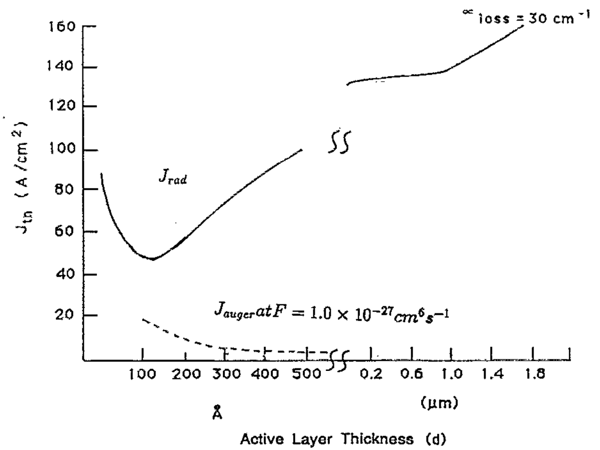

FIG. 5. Radiative and Auger currents at threshold as a function of active region thickness for the 2.5 μm laser.

From these measurements, the Auger lifetime is 300 ns at 77 K in a sample doped at 2.7×10^{15} cm^{-3}.[10] Using the relation

$$F\sim 1/t_{\text{Auger}}n_d^2, \tag{18}$$

we find a value of $F = 4.5 \times 10^{-25}$ cm^6 s^{-1}. Scaling this value with the band gap we obtain the following approximate values of F:

$$F(2.5\ \mu\text{m})=1.0\times10^{-27}\ \text{cm}^6/\text{s},$$

$$F(4.5\ \mu\text{m})=4.5\times10^{-26}\ \text{cm}^6/\text{s}. \tag{19}$$

The effects of varying F are clear since the Auger part of the current will vary linearly with the choice of F. The Auger current is

$$J_{\text{Auger}}=Fn_{3\text{D}}^3\, de, \tag{20}$$

where e is the electronic charge. The radiative current is

$$J_{\text{rad}}=eR_{\text{spon}}, \tag{21}$$

where R_{spon} is the spontaneous emission rate calculated at threshold densities. In Fig. 5, we show the radiative current and the Auger current as a function of the well size. Clearly the radiative current drops rapidly as the well size decreases. At very small well sizes the current starts to rise again when the *e*-*h* overlap starts to differ from unity, due to the wave-function leakage into the barrier region. The Auger current, however, increases as the well size decreases, because of the increase in $n_{3\text{D}}$. However, the Auger current is quite small even for the small well sizes. We can see that the total threshold current is a minimum for well sizes in the range of 100–200 Å. An important point is that small changes in the Auger coefficient F will not affect these results.

B. 4.5 μm case

In the discussion presented above for the 2.5 μm case, the conclusion that the quantum-well structure with thin active region has a lower threshold is quite independent of

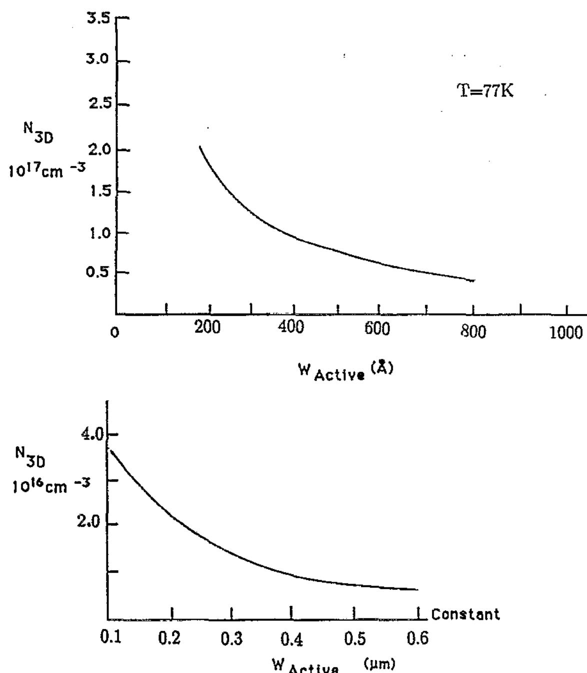

FIG. 6. Variation of the 3D carrier density at threshold as a function of active well size for the 4.5 μm laser.

the loss coefficient α_{loss}. For the 4.5 μm case, the Auger coefficient is considerably larger and dominates the laser performance of narrow-quantum-well devices as discussed below. For the results presented, we use a low value of 15 cm^{-1} for the cavity of loss. A higher loss will make the Auger effects even stronger, since the carrier density at threshold will be higher. A value of 15 cm^{-1} for cavity loss is probably the best that can be achieved at 4.5 μm. In Fig. 6 we show the dependence of the 3D carrier density for the 4.5 μm case on the active region thickness. As for the 2.5 μm case, the 3D carrier density increases rapidly when the active well size is decreased, as shown in Fig. 6. The difference in this case is that the Auger coefficient is quite large and the Auger current plays a much more important role in determining the threshold current. In Fig. 7 we show the radiative current at threshold along with the Auger current. The lowest threshold current does not occur for the quantum-well case, but for an active region of $\sim$0.1 μm.

We next examine the possibility of using multiquantum-well structures instead of a single-quantum-well structure to lower the threshold. In Fig. 8 we show the Auger and radiative currents for a 100 Å multiquantum well as a function of a number of wells. We note that while the current decreases, as the number of well sizes is increased, it is still much higher than the 0.1 μm active region value. Figure 9 shows results of a similar study done for 200 Å multiquantum wells. There is little advantage in using the multiple-quantum-well structure, although the threshold current is significantly lower than the current in the 100 Å case. Overall the 0.1 μm active region seems to be the best choice. Only if the Auger factor were 4–5 times

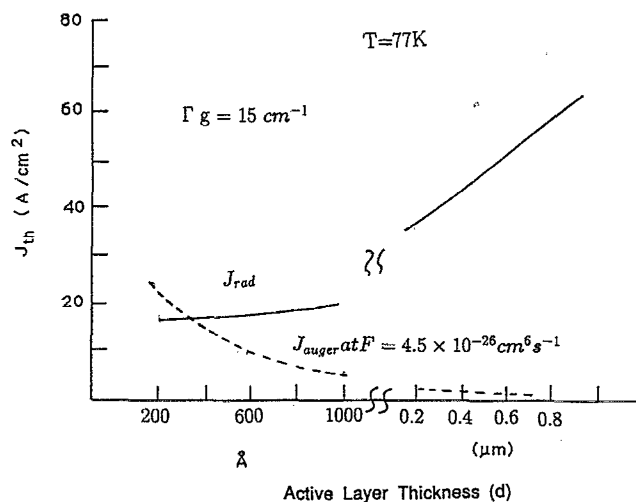

FIG. 7. Radiative current and Auger current at threshold as a function of active region thickness for the 4.5 μm laser.

smaller would it be advantageous to use the quantum-well structure for the 4.5 μm HgCdTe laser.

IV. CONCLUSIONS

In this paper we have examined the dependence of the radiative and Auger current at threshold for the 2.5 and 4.5 μm HgCdTe lasers at 77 K. For the 2.5 μm laser the results are similar in nature to those reported for the short-wavelength III-V semiconductor lasers, i.e., the threshold current is minimum for a narrow-quantum-well laser. The

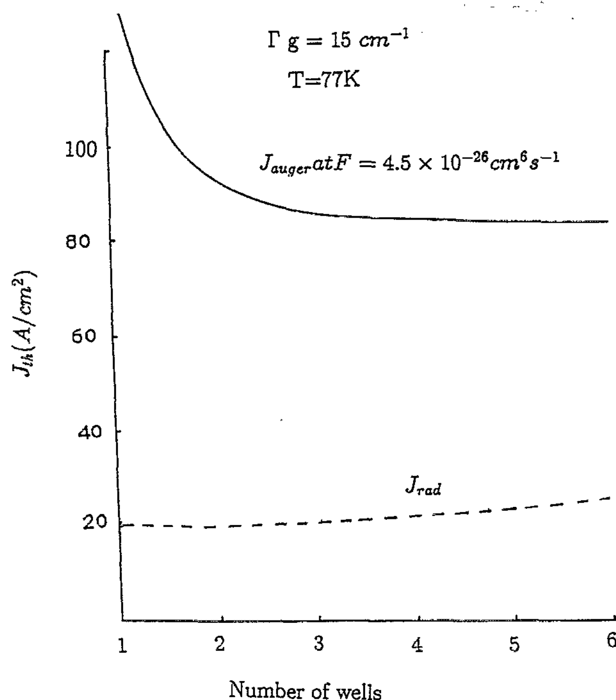

FIG. 8. Dependence of the Auger current and the radiative currents at threshold on the number of wells in a 100 Å multiquantum-well laser structure.

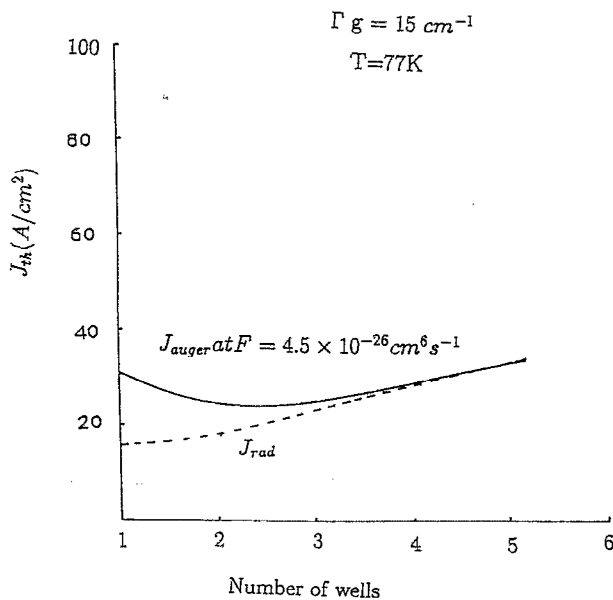

FIG. 9. Dependence of the Auger current and radiative currents at threshold on the number of wells in a 200 Å multiquantum-well laser structure.

optimum well size is 100–200 Å for the 2.5 μm case. However, for the 4.5 μm laser the results are quite different. The radiative current at threshold decreases with well size as in the case of the 2.5 μm case. However, the decrease is not as rapid because of the weaker optical confinement of the 4.5 μm laser. On the other hand, the Auger current increases rapidly as the well size decreases and starts dominating the radiative current for smaller active regions. The optimum active region is close to 0.1 μm for the 4.5 μm laser. This is an important conclusion because normally the laser performance improves as one goes to narrower-well lasers. This conclusion would also apply to lasers made with other semiconductors having zinc-blende structure, because the conclusions are dependent on the interplay of radiative and Auger processes. These processes are largely dependent on the band structure which is similar in materials with similar band gaps.

As the temperature is raised, the Auger current is expected to increase further. Thus for the 4.5 μm case, at higher temperatures the optimum width may be even larger than 0.1 μm.

ACKNOWLEDGMENTS

The authors thank their colleague J. M. Arias for valuable discussions. This work was supported by Phillips Laboratory under Contract No. F29601-90-C-0054.

[1] P. W. Kruse, Semicond. Semimet. **18**, 1 (1981).

[2] J. M. Arias, S. H. Shin, J. G. Pasko, R. E. DeWames, and E. R. Gertner, J. Appl. Phys. **65**, 1747 (1989); K. Vural, Opt. Eng. **26**, 201 (1987).

[3] M. Zandian, J. M. Arias, R. Zucca, R. V. Gil, and S. H. Shin, Appl. Phys. Lett. **59**, 1022 (1991).

[4] R. Zucca, M. Zandian, J. M. Arias, and R. V. Gil, J. Vac. Sci. Technol. B **10**, 1587 (1992).

[5] A. R. Beattie and P. T. Landsberg, Proc. R. Soc. London Ser. A **249**, 16 (1959).

[6] A. R. Beattie, J. Phys. Chem. Solids **49**, 589 (1988).

[7] A. Haug, J. Phys. Chem. Solids **49**, 599 (1988).

[8] H. Kressel and J. K. Butler, *Semiconductors and Heterojunction LEDs* (Academic, New York, 1977).

[9] J. P. Loehr and J. Singh, IEEE J. Quantum Electron. **QE-27**, 708 (1991).

[10] R. Zucca, D. D. Edwall, J. S. Chen, S. L. Johnston, and C. R. Younger, J. Vac. Sci. Technol. B **9**, 1823 (1991).